Rastislav BALON
Jan KOMENDA

ANALYSIS OF THE 155 MM ERFB/BB PROJECTILE TRAJECTORY

Reviewer: Jan KUSÁK

A b s t r a c t :

The article is focused on the external-ballistic analysis of the 155 mm artillery High-Explosive Extended-Range Full-Bore projectile with the Base Burn Unit (ERFB/BB), designed for the Slovak 155 mm Self-Propelled Gun Howitzer ZUZANA. The external-ballistic analysis of the characteristics of the 155 mm ERFB/BB shell is made for the Modified Point Mass Trajectory Model with additional terms for the Base Burn projectiles – Method 1 (MPMM+BB1) which is standardized in the STANAG 4355 agreement. The aim of this analysis is to determine all required data for the trajectory model mentioned above, specifically dimensional and mass properties, aerodynamic data, ballistic data and also the Base Burn Unit data. The results of the theoretical analysis are compared with the results of experimental firing tests.

List of Abbreviations

BB	- Base Burn (Base Bleed)
BT	- Boat Tail
CAD	- Computer Aid Design
ERFB	- Extended Range Full Bore
MPMM	- Modified Point Mass Model

MPMM+BB1 - MPMM model with additional terms for Base Burn projectiles – Method 1
PMM - Point Mass Model
SPGH - Self-Propelled Gun Howitzer

List of main Symbols

d [m] - Reference diameter of the projectile
$\vec{g}$ [$m.s^{-2}$] - Vector of acceleration due to gravity
i [-] - Form factor
i_{BB} [-] - Fitting factor to adjust the drag reduction as a function of a quadrant elevation
m [kg] - Fuzed projectile mass at time t
$\dot{m}_f$ [$kg.s^{-1}$] - Mass flow rate of the base burn unit fuel
mil - Planar angle unit for which is stated: 6400 *mil* = 6000 *dc* = 2π *rad* = 360°
$\vec{p}$ [$rad.s^{-1}$] - Vector of the axial spin rate of the projectile
t [s] - Computation time of flight
$\vec{u}$ [$m.s^{-1}$] - Vector of velocity of the projectile wrt ground-fixed axes
$\vec{v}$ [$m.s^{-1}$] - Vector of velocity of the projectile wrt air
$\vec{w}$ [$m.s^{-1}$] - Vector of velocity of the air wrt ground-fixed axes (wind velocity)
$\vec{1}, \vec{2}, \vec{3}$ - Base vectors of the ground-fixed coordinate system
1, 2, 3 - Vector components indexes (1- in range, 2- in altitude, 3- in side)
A_D [*mil*] - Drift
A_ω [°] - Angle of fall
$\overrightarrow{BBF}$ [N] - Vector of the force due to base burn
C [-] - Aerodynamic coefficient
$\overrightarrow{DF}$ [N] - Vector of the drag force
$\overrightarrow{CF}$ [N] - Vector of the Coriolis force
$\overrightarrow{GF}$ [N] - Vector of the gravity force
I_x [$kg.m^2$] - Axial moment of inertia of the projectile
I_y [$kg.m^2$] - Transversal moment of inertia of the projectile
$\overrightarrow{LF}$ [N] - Vector of the lift force
$\overrightarrow{MF}$ [N] - Vector of the Magnus force
M [-] - Mach number
MT [°] - Temperature of the base burn unit fuel
$\overrightarrow{OM}$ [$N.m$] - Overturning moment
P [Pa] - Air pressure

$QE\ [mil]$ - Quadrant elevation
$T\ [s]$ - Time of flight
$U\ [m.s^{-1}]$ - Standard muzzle velocity
$V_C\ [m.s^{-1}]$ - Burning rate of the base burn unit fuel
$V_\omega\ [m.s^{-1}]$ - Velocity at graze (remaining velocity)
$X\ [m]$ - Range (in table of the trajectory elements)
$\vec{X}\ [m]$ - Position vector of the center of mass of the projectile wrt ground-fixed axes
$X_{2M}\ [m]$ - Height of a muzzle of the barrel above the mean sea level
$Y_S\ [m]$ - Trajectory vertex height
$\vec{\alpha}_e\ [rad]$ - Vector of yaw of repose approximation
$\rho\ [kg.m^{-3}]$ - Air density
$\rho_p\ [kg.m^{-3}]$ - Density of the base burn unit fuel
$\vec{\omega}\ [rad.s^{-1}]$ - Angular velocity vector of the coordinate system due to the angular speed of the Earth
$\vec{A}\ [m.s^{-2}]$ - Vector of acceleration due to the Coriolis effect

1. Introduction

The 155 mm ERFB/BB shell, analyzed in this article, is the latest type of the shell for the Self-Propelled Gun Howitzer (SPGH) ZUZANA. This weapon system was developed by the company Konštrukta-Defence a.s. Trenčín, Slovak Republic and became a contemporary artillery mean of the Slovak Armed Forces. Long firing range of this system (approximately 39 km with the 155 mm ERFB/BB shell fired from the 45-caliber-long barrel) is mostly achieved by slender shell body geometry and a base drag reduction by using the base burn unit[1].

Since joining the Slovak Republic to the NATO alliance, an implementation of the trajectory models standardized in NATO has become required. The company Konštrukta-Defence a. s. plays an important role in the implementation of the NATO trajectory models and their application on the 155 mm caliber shells.

2. Description of ammunition with the 155 mm ERFB/BB projectile

The ammunition with 155 mm ERFB/BB projectile is designed as a separate loaded, i.e. the projectile and the propelling charge are loaded separately into the chamber. The primer IN-97 is used for initiation of the propelling charge. The primer is automatically inserted into the breech-block just before the fire.

[1] also known as base-bleed unit

2.1. ERFB/BB projectile

155 mm ERFB/BB (Fig. 1) is a high explosive Extended Range (ER) Full Bore (FB) projectile with the base burn (BB) unit assistance. The projectile has a long front ogive which continuously passes through a short cylindrical part of the bourrelet to the base part of the projectile created by the base burn unit (base burn motor). The driving band is made of a copper alloy and placed into the groove just behind the cylindrical bourrelet at the transition point from the front ogive to the rear ogive. At the nose of the projectile, there is a mechanical point detonating fuze with an immediate and/or delay function screwed on the projectile body (some of the M557, M739 and KZ-984 fuzes can be used).

A steel body of the base burn unit creates a rear ogive in the form of a truncated cone with the inclination angle of 3° of surface line with respect to longitudinal axis (also named "tail angle"). The body of the base burn unit is filled with a solid fuel of the type **I-A-4**. Driving of the projectile in the barrel is provided by the rear cylindrical bourrelet placed near the driving band and four front bourrelet segments, known as "bourrelet nubs", placed on the front ogive.

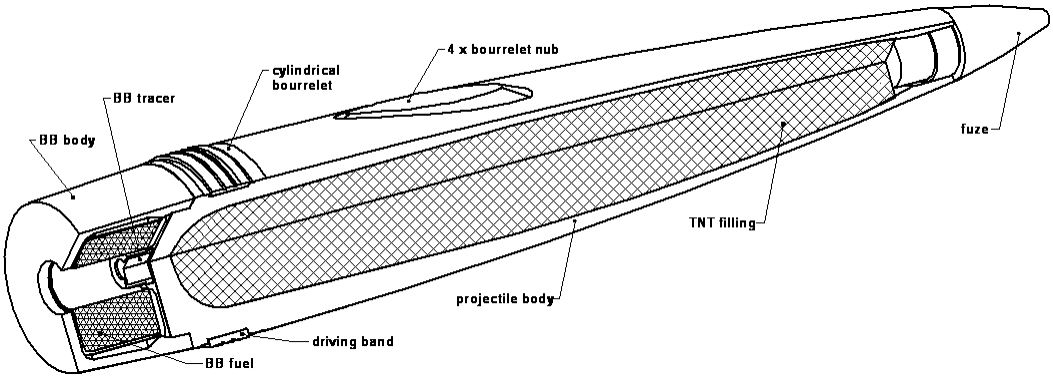

Fig. 1 155 mm ERFB/BB projectile

2.2. Uncased modular propelling charges

A combination of the modular propelling charges A+A+B or long-range single-increment propelling charge D are designed for assembling the ammunition with 155 mm ERFB/BB projectile (Fig. 2). All propelling charges are uncased and combustible (manufacturer Explosia a.s., Pardubice, Czech Republic). The modular propelling charges A+A+B consist of a single-base seven-hole propellant and a specific central igniter, all contained in a combustible case. The propelling charge D is composed of a combustible case which contains a triple-base stick propellant, base igniter, wear-reducing additive and a flash reducer. Other incremental propelling

charges combined from the modules A and B (for example charges A, B, A+B) are not used for firing with the 155 mm ERFB/BB projectile from the SPGH Zuzana.

The 155 mm ERFB/BB projectile fired from the SPGH Zuzana barrel (45-calibers-long, constant twist of rifling t_c = 20 *calibers/rev*) obtains at standard conditions (propellant temperature 21 °*C*, reference projectile mass, no barrel wear) the following standard muzzle velocity *U*: charge A+A+B: 620 $m.s^{-1}$; charge D: 908 $m.s^{-1}$.

3. Modified point mass trajectory model (MPMM+BB1)

The Modified Point Mass Trajectory Model with additional terms for the Base Burn projectiles – Method 1, designated as MPMM+BB1, is a trajectory model intended for the spin-stabilized Base Burn projectiles. The model is standardized in the NATO alliance by the STANAG 4355 agreement. The core of this model is created by the Modified Point Mass Trajectory Model (MPMM). It enables to solve a position of the center of mass of the projectile (coordinates X_1, X_2, X_3) with 3 degrees of freedom like a simple Point Mass Trajectory Model (PMM). The modification of a simple Point Mass Trajectory Model is obtained by computation of the yaw of repose approximation α_e (i.e. 4th degree of freedom) from the amount equality of aerodynamic overturning moment *OM* and gyroscopic moment caused by the rotation of the projectile along its longitudinal axis.

Applicability of the model MPMM is limited only for spin-stabilized projectiles. Apart from the basic forces acting on the projectiles considered in the model PMM (*drag force* $\overrightarrow{DF}$, *gravity force* $\overrightarrow{GF}$ and *Coriolis force* $\overrightarrow{CF}$) the model MPMM enables by knowledge of the yaw of repose approximation to include the additive aerodynamic forces influence (*lift force* $\overrightarrow{LF}$, *Magnus force* $\overrightarrow{MF}$) into the equation of motion. In the model with additional terms for the Base Burn projectiles – Method 1, there is a base drag reduction caused by the base burn unit which is expressed by the force $\overrightarrow{BBF}$ which acts in the direction of the longitudinal projectile axis, from its base to the nose (Fig. 3).

According to [5], the equation of motion of the center of mass of the projectile with an actual mass *m* and velocity $\vec{u}$ for the model MPMM+BB1 has the following form:

$$m\dot{\vec{u}} = \overrightarrow{GF} + \overrightarrow{DF} + \overrightarrow{LF} + \overrightarrow{MF} + \overrightarrow{CF} + \overrightarrow{BBF} \,. \tag{1}$$

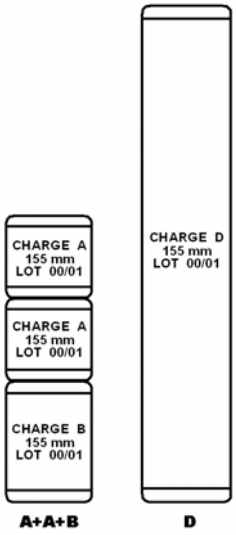

Fig. 2 Propelling charges for 155 mm ERFB/BB projectile

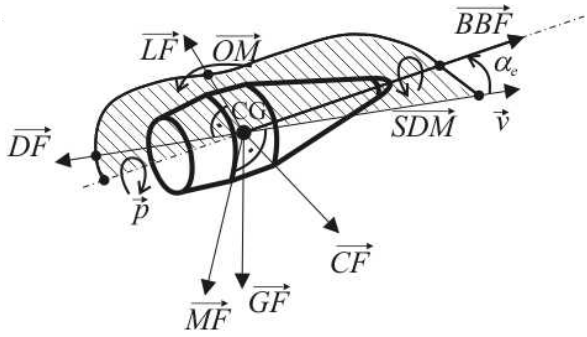

Fig. 3 Forces and moments acting on the projectile (MPMM+BB1 model)

Gravity force

Gravity force is stated by equation:

$$\overrightarrow{GF} = m.\vec{g} \ , \tag{2}$$

where:

$\vec{g}$ - acceleration due to gravity,

m - actual mass of the projectile.

Drag force

Drag force $\overrightarrow{DF}$ is a basic force which influences the projectile motion on its trajectory. The vector of the relative velocity of the projectile with respect to air $\vec{v}$ does not lie in the longitudinal axis of the projectile due to air side-flow. Vector $\vec{v}$ and the longitudinal axis of the projectile form the yaw angle α_e (Fig. 4) in the **drag plane**. Then, it is possible to express the drag force in the model with 4 degrees of freedom according to [5] by equation:

$$\overrightarrow{DF} = -\left(\frac{\pi \rho i d^2}{8}\right)\left(C_{D_o} + C_{D_{\alpha^2}}\left[Q_D \alpha_e\right]^2\right) v \vec{v} \ , \tag{3}$$

where:

ρ - local air density,
d - reference diameter of the projectile,
α_e - yaw of repose approximation,
$\vec{v}$ - vector of relative velocity of the projectile with respect to air, $\vec{v} = \vec{u} - \vec{w}$,
$\vec{u}$ - vector of velocity of the projectile, $\vec{u} = \dot{\vec{X}}$,
$\vec{X}$ - position vector of the center of mass of the projectile wrt ground-fixed axes,
$\vec{w}$ - vector of velocity of the air (wind velocity),
C_{D_o} - zero yaw drag coefficient,
$C_{D_{\alpha^2}}$ - quadratic yaw drag coefficient,
i - form factor of the projectile,
Q_D - yaw drag fitting factor.

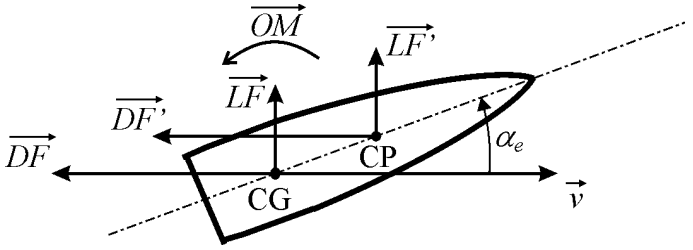

Fig. 4 Drag and lift forces acting on the projectile in the drag plane
CG – center of mass of the projectile, CP – center of pressure

Equation (3) of the model MPMM enables by $C_{D_{\alpha^2}}$ coefficient to compute the yaw drag induced by the yaw of repose α_e.

Lift force

By reason of the projectile axis yawing from the direction of the vector of relative velocity $\vec{v}$, there is a resulting lift force $\overrightarrow{LF}$ which is stated according to [5] by a formula:

$$\overrightarrow{LF} = \left(\frac{\pi \rho d^2 f_L}{8} \right) \left(C_{L_\alpha} + C_{L_{\alpha^3}} \alpha_e^2 \right) v^2 \vec{\alpha}_e \quad , \tag{4}$$

where:

$\vec{\alpha}_e$ - vector of yaw of repose approximation,

C_{L_α} - lift force coefficient,

$C_{L_{\alpha^3}}$ - cubic lift force coefficient,

f_L - lift factor.

Lift force $\overrightarrow{LF}$ is perpendicular to a drag force $\overrightarrow{DF}$'. Both forces $\overrightarrow{DF}$' and $\overrightarrow{LF}$' lie in the drag plane and act on the projectile in the common point CP called the **center of pressure**. Since the point CP is not identical with the center of mass of the projectile CG (for spin-stabilized artillery projectiles the point CP is placed more closely to the nose than CG) the aerodynamic forces $\overrightarrow{DF}$' and $\overrightarrow{LF}$' result in an overturning moment $\overrightarrow{OM}$ which has a rotating effect around the center of mass of the projectile CG. Forces $\overrightarrow{DF}$' and $\overrightarrow{LF}$' are identically substituted both in magnitude and direction by forces $\overrightarrow{DF}$, $\overrightarrow{LF}$ acting in the center of mass CG. Destabilizing effect of the overturning moment $\overrightarrow{OM}$ is compensated by the gyroscopic moment caused by the rotation of the projectile along its longitudinal axis.

Magnus force

The Magnus force is a result of a simultaneously acting air side-flow and a rotation of the projectile along its longitudinal axis with a spin rate $\vec{p}$. According to [5], it is expressed by the following formula:

$$\overrightarrow{MF} = -\frac{\pi \rho d^3 Q_M \; p C_{mag-f}}{8} \left(\vec{\alpha}_e \times \vec{v}\right) , \tag{5}$$

where:

p - axial spin rate of the projectile,

C_{mag-f} - Magnus force coefficient,

Q_M - Magnus fitting factor.

Velocity of the air side-flow is expressed in the equation (5) as a vector product of the yaw of repose approximation and the relative velocity of the projectile wrt air $\vec{\alpha}_e \times \vec{v}$.

Coriolis force

Coriolis force caused by the Earth rotation around its axis is defined as:

$$\overrightarrow{CF} = m.\vec{\Lambda}\,, \tag{6}$$

where:

$\vec{\Lambda}$ - vector of acceleration due to the Coriolis effect, $\vec{\Lambda} = -2\,(\vec{\omega} \times \vec{u})$,

$\vec{\omega}$ - angular velocity vector of the coordinate system due to the angular speed of the Earth.

Force due to base burn

Used trajectory model includes the effect of the base burn unit using the additional driving force which acts in the longitudinal projectile axis direction (as well as a rocket motor thrust force of the rocket-assisted projectiles). This force is stated according to [5] as follows:

$$\overrightarrow{BBF} = +\frac{\pi\,\rho\,i_{BB}\,d^2}{8}\,f(I)\;C_{x_{BB}}\;v^2\left(\frac{\vec{v}\cos\alpha_e}{v} + \vec{\alpha}_e\right), \tag{7}$$

where

$C_{x_{BB}}$ - drag reduction coefficient during the base burn unit burning,

i_{BB} - fitting factor to adjust the drag reduction as a function of a quadrant elevation,

$\dot{m}_f$ - mass flow rate of the base burn unit fuel, $\dot{m} = -\dot{m}_f$,

d_b - diameter of the projectile base,

I - base burn unit fuel injection parameter for which is given as follows:

$$I = \frac{4\,\dot{m}_f}{\pi\,d_b^2\;\rho\,v}\,, \tag{8}$$

$f(I)$ - the characteristic flow rate function of the base burn unit for which is given:

$$f(I) = \frac{I}{I_0} \qquad \text{for} \quad I < I_0\,, \tag{9}$$

$$f(I) = 1 \qquad \text{for} \quad I \geq I_0\,, \tag{10}$$

I_0 - base burn unit fuel injection parameter for the optimum efficiency which is the function of the Mach number *M*.

The computation of the force $\overrightarrow{BBF}$ caused by the base burn unit is similar as a drag force $\overrightarrow{DF}$ computation according to the equation (3). The $\overrightarrow{BBF}$ force is expressed by aerodynamic coefficient $C_{x_{BB}}$ which is the function of the Mach number *M*. Mass flow intensity of the base burn unit fuel is characterized by the non-dimensional base burn unit fuel injection parameter *I*. If the base burn unit fuel injection parameter *I* doesn't reach the optimal value I_0 then the force $\overrightarrow{BBF}$ in the equation (7) is reduced by the characteristic flow rate function $f(I)$ according to equation (9). In the case when the base burn unit fuel injection parameter *I* reaches or exceeds the optimal value I_0 then the characteristic flow rate function $f(I)$ according to equation (10) does not influence the $\overrightarrow{BBF}$ force. Force *BBF* = 0 after burning out of the the base burn unit fuel. Mass flow rate of the fuel is given during the base burn unit fuel burning by formula:

$$\dot{m}_f = -V_C \, \rho_p \, S_C(m_{CB}), \tag{11}$$

where

ρ_p - density of the base burn unit fuel,

S_C - burning surface of the base burn unit fuel at time *t*, expressed as a function of the mass of fuel burnt m_{CB},

m_{CB} - mass of the base burn unit fuel burnt, $m_{CB} \in \langle 0, m_f \rangle$,

m_f - base burn unit fuel mass,

V_C - burning rate of the base burn unit fuel, V_C is given as follows:

$$V_C = V_{C_0} \, (e^{\beta(MT-21°C)}) \, (k \, P^n) \, K(p), \tag{12}$$

where:

$K(p)$ - function which takes into account the influence of the axial spin rate *p* of the projectile on the burning rate, $K(p)$ is a linear function as follows:

$$K(p) = a_0 + a_1 p, \tag{13}$$

V_{C_0} - burning rate obtained on the strand burner at a standard pressure and temperature,

MT - base burn unit fuel temperature (in degrees of centigrade),

β - base burn unit temperature fuel burning coefficient,

k, n - coefficients in burning rate versus the pressure formula,

P - local air pressure,

a_0, a_1 - coefficients in burning rate versus the spin rate formula $K(p)$,
p - axial spin rate of the projectile.

Equation (12) takes into account the influence of base burn unit fuel temperature *MT*, air pressure *P* and a projectile spin rate *p* on the burning rate V_C and on the mass flow rate intensity of the base burn unit fuel. Considering that β, n and a_1 coefficients have a positive value, the increase of fuel temperature *MT*, air pressure *P* and projectile spin rate *p* causes the increase of the burning rate of the base burn unit fuel V_C.

The **spin acceleration of the projectile** $\dot{p}$ is proportional to the aerodynamic spin damping moment *SDM* according to [5] as follows:

$$\dot{p}\, I_x = SDM = \frac{\pi \rho\, d^4}{8}\, p\, v\, C_{spin}\ , \tag{14}$$

C_{spin} - spin damping moment coefficient,
I_x - axial moment of inertia of the projectile.

The **yaw of repose approximation vector** $\vec{\alpha}_e$ has an identical direction and orientation as a lift force vector $\overrightarrow{LF}$. Angle α_e does not express the immediate value of the yaw angle which the projectile has in a specific point during the flight, but expresses its approximate value. The yaw of repose approximation vector $\vec{\alpha}_e$ is computed according to [5] by the vector equation based on the amount equality of an aerodynamic overturning moment *OM* and a gyroscopic moment caused by the rotation of the projectile along its longitudinal axis:

$$\vec{\alpha}_e = -\frac{8\, I_x\, p\left(\vec{v} \times \dot{\vec{u}}\right)}{\pi \rho\, d^3\, (C_{M_\alpha} + C_{M_{\alpha^3}} \alpha_e^2)\, v^4}\ , \tag{15}$$

C_{M_α} - overturning moment coefficient,
$C_{M_{\alpha^3}}$ - cubic overturning moment coefficient.

All of the aerodynamic forces and moments considered above, except the Coriolis and gravity force, (i.e. drag force $\overrightarrow{DF}$, lift force $\overrightarrow{LF}$, Magnus force $\overrightarrow{MF}$, force due to the base burn $\overrightarrow{BBF}$, spin damping moment $\overrightarrow{SDM}$, overturning moment $\overrightarrow{OM}$) are expressed by **dimensionless aerodynamic coefficients** *C*.

In the aerodynamic forces expressions there are included non-dimensional coefficients - factors in order to create a correspondence between the computed and the observed range testing results. These factors are designated together as **ballistic**

fitting factors. The application of the fitting factors enables to compensate for the approximation in the equation of motion, aerodynamic coefficients, projectile and the base burn unit performance.

In the trajectory model MPMM+BB1 there are the following ballistic fitting factors:

- i - form factor of the projectile in the model MPMM; i fits the range, but in the model MPMM+BB1 with additional terms for the Base Burn projectiles is fixed $i = 1$,
- i_{BB} - factor to adjust the drag reduction; i_{BB} fits the range,
- f_L - lift factor, f_L fits the side coordinate of the projectile graze,
- Q_D - yaw drag fitting factor, Q_D fits the range in high angles of a quadrant elevation,
- Q_M - Magnus fitting factor, Q_M fits the trajectory vertex height and the time of flight.

According to experiences of the MPMM+BB1 model users, it is normally chosen either $Q_D = Q_M = 1.0$ (French model) or $Q_D = Q_M = 1.2$ (US model) and the total trajectory model is fitted by i_{BB} and f_L factors analyzed from the range testing results. Besides the mentioned fitting factors, the time of base burn unit ignition delay t_{DI} [s] belongs to ballistic data too. t_{DI} defines the time which elapses from the moment when a projectile leaves the muzzle to the moment of the base burn unit fuel ignition. The t_{DI} depends on the base burn unit construction and normally is included in the interval <0, 1> s.

All vectors of the trajectory model have as a frame of reference a right-handed, orthonormal, Cartesian, **ground-fixed coordinate system** (*O, 1, 2, 3*) with the base vectors $\vec{1}, \vec{2}, \vec{3}$. The origin *O* is the point where the local vertical line, perpendicular to surface of geoid, through the weapon muzzle, intersects the geoid. The axis *1* is the intersection of the vertical plane of fire and the horizontal plane going through the origin *O*. The axis *1* is pointing in the direction of fire. The axis *2* is parallel to the gravity acceleration vector $\vec{g}$ and opposite in direction. The axis *3* completes the right-handed coordinate system.

The trajectory model equation of motion (2) is solved by the numerical integration for **initial conditions** in the form:

$$\vec{X}_o = \vec{X}_{(t=0)} = \begin{bmatrix} 0 \\ X_{2M} \\ 0 \end{bmatrix}, \quad \vec{u}_o = \vec{u}_{(t=0)} = \begin{bmatrix} u_o \cos(QE) \\ u_o \sin(QE) \\ 0 \end{bmatrix}, \tag{16}$$

X_{2M} - height of a muzzle of the barrel above the mean sea level,

QE^2 - quadrant elevation,

u_o - initial velocity of the projectile with respect to ground-fixed axes.

All data required by the trajectory model (dimensional, mass, aerodynamic, ballistic and base burn unit data) for the 155 mm ERFB/BB projectile are stated in the following sections.

4. Trajectory model inputs

4.1. Dimensional and mass data

The following table lists necessary and informative data (from the considered MPMM+BB1 trajectory model view) for the 155 mm ERFB/BB projectile.

necessary data	reference diameter of the projectile	d	m	0,155
	diameter of the projectile base	d_b	m	0,1409
	fuzed projectile mass, initially	m_o	kg	47,5
	axial moment of inertia of the projectile, initially	I_{x_o}	$kg.m^2$	0,161
	distance of the center of mass of the projectile from the nose, initially	X_{CG_o}	m	0,6287
	axial moment of inertia of the projectile at BB unit burnout	I_{x_B}	$kg.m^2$	0,1592
	distance of the center of mass of the projectile from the nose at BB unit burnout	X_{CG_B}	m	0,6236
informative data	overall fuzed projectile length	-	m	0,9487
	forward ogival length	-	m	0,7714
	cylindrical length	-	m	0,0683
	tail length	-	m	0,1090
	transversal moment of inertia of the projectile, initially	I_{y_o}	$kg.m^2$	2,1061
	transversal moment of inertia of the projectile at BB unit burnout	I_{y_B}	$kg.m^2$	2,0367

Tab. 1 Dimensional and mass data for the 155 mm ERFB/BB projectile

[2] In accordance with STANAG 4355, the quadrant elevation *QE* substitutes the angle of departure Θ_o in the equation (16). With respect to the real value of the jump angle the range is fitted by form factor *i*.

4.2. Aerodynamic data

Aerodynamic properties of the 155 mm ERFB/BB projectile were predicted by the commercial software PRODAS V3 created by the company Arrow Tech Associates, USA. The mentioned software works on the algorithm base using semi-empirical formulations. These semi-empirical formulations were formed on the base of aerodynamic data measured for the various types of projectiles. In the PRODAS software, there is initially created a projectile model, which dimensional and mass properties correspond to the real projectile. PRODAS software predicts all set of required aerodynamic data after creating the projectile model. The values of aerodynamic coefficients predicted by PRODAS software for the 155 mm ERFB/BB projectile with inert base burn unit are listed in Tab. 2.

M	C_{D_o}	$C_{D_{\alpha^2}}$	C_{L_α}	$C_{L_{\alpha^3}}$	C_{mag-f}	C_{M_α}	C_{spin}
0.400	0.138	4.1710	1.302	20	-0.510	3.725	-0.01320
0.600	0.138	4.1710	1.302	20	-0.510	3.733	-0.01320
0.700	0.139	4.4305	1.311	20	-0.510	3.849	-0.01280
0.750	0.140	4.5500	1.430	20	-0.510	4.220	-0.01260
0.800	0.141	4.6895	1.439	20	-0.510	4.276	-0.01240
0.850	0.148	4.9560	1.452	20	-0.545	4.553	-0.01210
0.875	0.152	5.0840	1.458	20	-0.560	4.692	-0.01195
0.900	0.156	5.2320	1.474	20	-0.575	4.830	-0.01180
0.925	0.177	5.4915	1.423	20	-0.650	4.686	-0.01170
0.950	0.199	5.7505	1.371	20	-0.725	4.542	-0.01155
0.975	0.244	6.0280	1.436	20	-0.695	4.565	-0.01155
1.000	0.290	6.2950	1.490	20	-0.665	4.587	-0.01150
1.025	0.309	6.5755	1.551	20	-0.635	4.522	-0.01160
1.050	0.329	6.8555	1.621	20	-0.605	4.457	-0.01175
1.100	0.326	7.4470	1.694	20	-0.575	4.516	-0.01150
1.200	0.318	8.0510	1.802	20	-0.510	4.572	-0.01150
1.350	0.305	7.6075	1.945	20	-0.510	4.599	-0.01130
1.500	0.291	7.1545	2.089	20	-0.510	4.708	-0.01110
1.750	0.269	6.7155	2.251	20	-0.510	4.723	-0.01100
2.000	0.249	6.2655	2.411	20	-0.510	4.649	-0.01110
2.250	0.233	6.0135	2.517	20	-0.510	4.613	-0.01105
2.500	0.216	5.7620	2.614	20	-0.510	4.573	-0.01100
3.000	0.194	5.2330	2.576	20	-0.510	4.327	-0.01070
3.500	0.176	4.9720	2.544	20	-0.510	4.289	-0.01065

Tab. 2 Aerodynamic coefficients C vs. Mach number M relationship for the 155 mm ERFB/BB projectile with the inert base burn unit

The drag force $\overrightarrow{DF}$ is the most significant aerodynamic force acting on the projectile which causes deceleration of the projectile on its trajectory. The drag force for the well stabilized projectile (yaw angle $\alpha_e < 3°$) depends mainly on the zero yaw drag coefficient value C_{D_o} according to equation (3). The C_{D_o} coefficient for the 155 mm ERFB/BB projectile is plotted against Mach number M in Fig. 5. For comparison, there is also included in the Fig. 5 the C_{D_o} coefficient for the etalon projectile of the Soviet Drag Law from 1943 which has been used in external ballistics of artillery projectiles by countries of the former Eastern block.

The base drag reduction effect caused by the base burn unit fuel ejection is expressed in the MPMM+BB1 trajectory model by the drag reduction coefficient $C_{x_{BB}}$ according to the equation (7). The drag reduction coefficient $C_{x_{BB}}$ was software predicted like other aerodynamic coefficients. The $C_{x_{BB}}$ versus Mach number relationship is shown in Fig. 6. Related function of the base burn unit fuel injection parameter for the optimum efficiency I_0 is shown in Fig. 7.

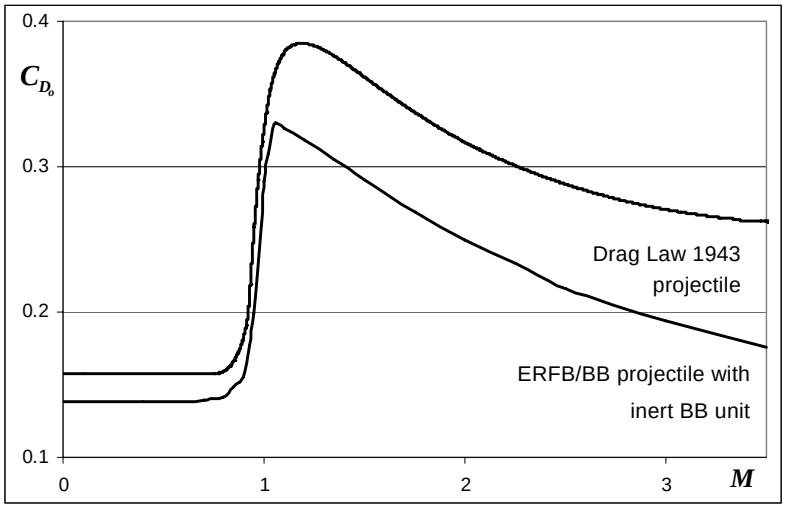

Fig. 5 C_{D_o} aerodynamic coefficient relationship

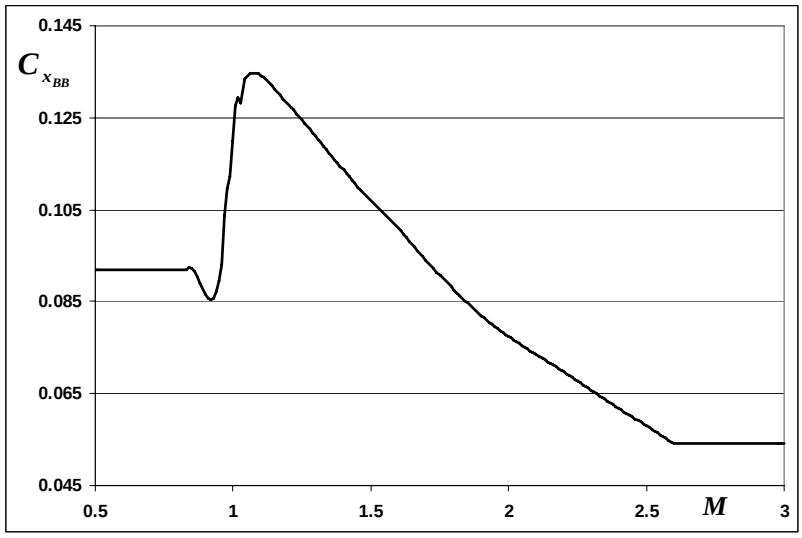

Fig. 6 $C_{x_{BB}}$ vs. Mach number M relationship for the 155 mm ERFB/BB projectile

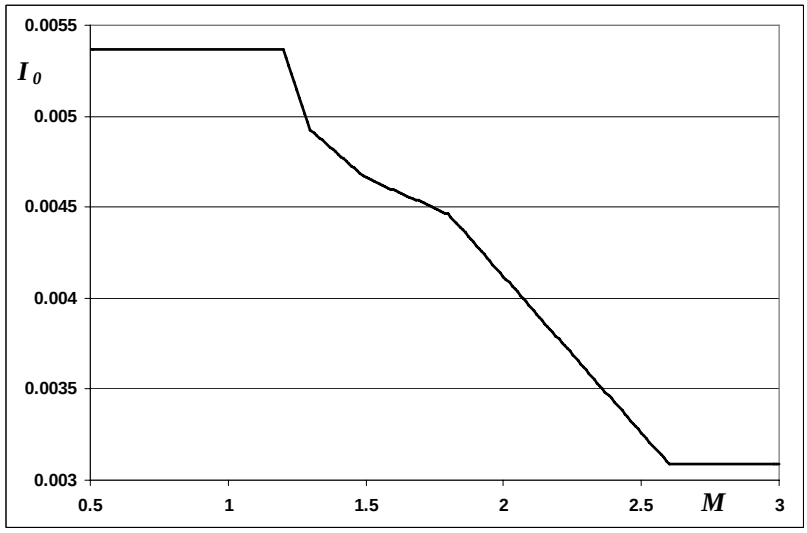

Fig. 7 I_0 vs. Mach number M relationship for the 155 mm ERFB/BB projectile

4.3. Base burn unit data

The 155 mm ERFB/BB projectile uses the base burn unit filled with **I-A-4** solid fuel which is produced by the Dutch company Muiden Chemie International. The base burn unit properties stated from the producer data are listed in Tab. 3.

base burn unit fuel mass	m_f	kg	0.88
the smallest thickness of the base burn unit solid fuel	e_1	m	0.03655
density of the base burn unit fuel	ρ_p	$kg.m^{-3}$	1548
standard burning rate of the base burn unit fuel	V_{C_0}	$m.s^{-1}$	0.8337E-3
base burn unit temperature fuel burning coefficient	β	-	2.12229E-3
exponent in burning rate versus pressure formula	n	-	7.685E-1
constant in burning rate versus pressure formula	k	-	1.539E-4

Base burn unit burning time T_{BB} vs spin rate p tabular relationship and related values of the $K(p)$ function for standard conditions 21°C a 1013 *hPa*.

p [$rad.s^{-1}$]	T_{BB} [s]	$K(p)$ [-]
0.00	40.53	1.00000
622.04	32.32	1.25392
892.21	29.38	1.37931
1105.84	27.76	1.45985
1250.35	26.34	1.53846
1420.00	24.21	1.67364
1589.65	23.10	1.75439

Tab. 3 Base burn unit data for the 155 mm ERFB/BB projectile

The required linear function $K(p) = a_0 + a_1\, p$, where a_0 = 0.97283 and $a_1 = 4.72.10^{-4}$ (Fig. 8), is stated by approximation of values of the $K(p)$ function listed in Tab. 3 and takes into account the influence of axial spin rate p of the projectile on the burning rate V_C of the base burn unit fuel. From the stated relationship results that the burning rate of the base burn unit fuel raises with the raising spin rate of the projectile.

The burning surface of the base burn unit fuel is expressed as a function of the mass of the fuel burnt m_{CB}: $S_C = a_i + b_i\, m_{CB}$ where $m_{CB_i} \le m_{CB} \le m_{CB_{i+1}}$. This relationship was stated numerically by CAD software I-DEAS where values of the burning surface S_C and related values of the mass of the fuel burnt m_{CB} were computed for discreetly chosen values of the thickness of the base burn unit solid fuel model. The obtained relationship $S_C(m_{CB})$ is shown in Fig. 9.

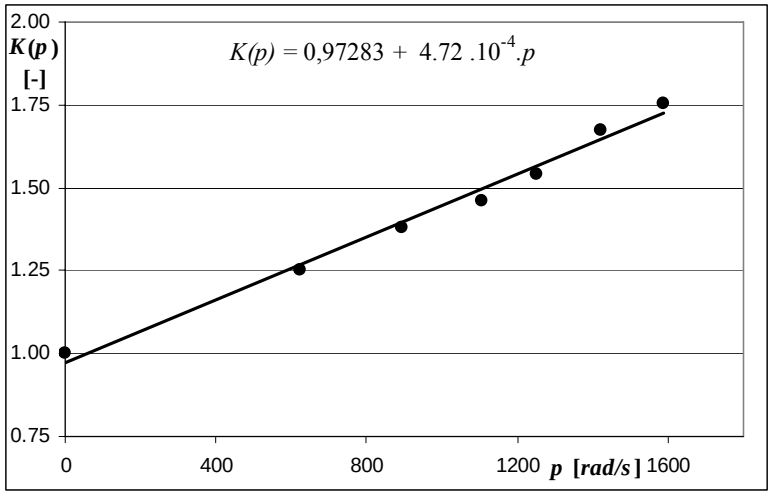

Fig. 8 Function $K(p)$ which takes into account the influence of axial spin rate p of the projectile on the burning rate of the base burn unit fuel

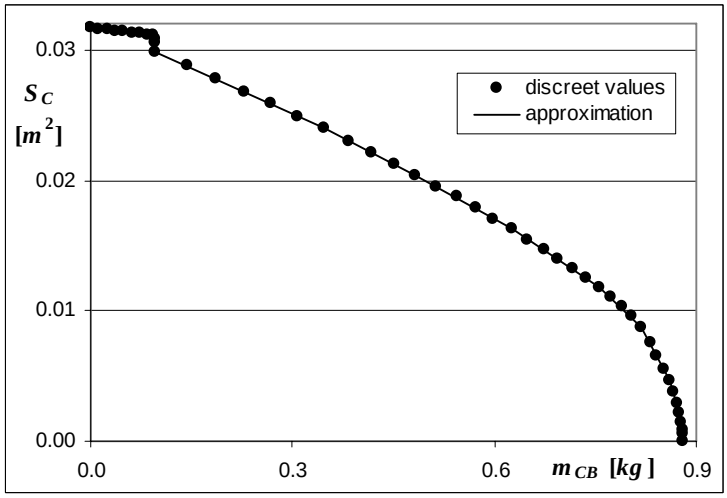

Fig. 9 Area of combustion of the base burn unit fuel S_C as a function of the mass of the fuel burnt m_{CB}

Besides the base burn unit data mentioned above, it is needed for the MPMM+BB1 model to know the mass m_{CB_0} of the base burn unit fuel burnt in the barrel. The mass m_{CB_0} is stated for the 155 mm ERFB/BB projectile by numerical integration of the mass flow rate of the base burn unit fuel, equation (11), during the internal-ballistic

process in the barrel. The computation was made on the basis of the propellant gas pressure curve measured in the barrel during the 155 mm ERFB/BB projectile fire with the propelling charge D. Two KISTLER 6213B piezoelectric gauges were used for the measurement. Time relation of the mean propellant gas pressure (transformed to the projectile base) obtained from these gauges is shown in Fig. 10. The computed mass m_{CB_0} of the base burn unit fuel burnt in the barrel is of 0.06 *kg*, i.e. 6.8 % from the overall base burn unit fuel mass m_f.

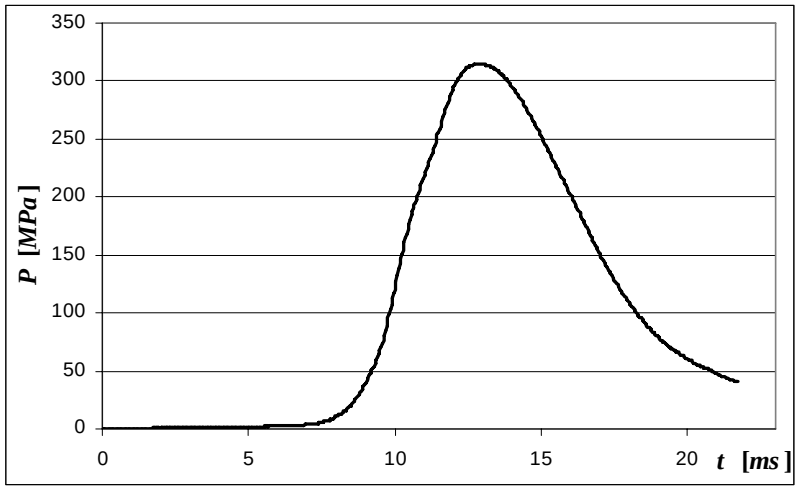

Fig. 10 Propellant gas pressure curve transformed to the projectile base for the 155 mm ERFB/BB projectile with propelling charge D

4.4. Ballistic data

The function of the 155 mm ERFB/BB projectile in configuration with propelling charges A+A+B and D was verified by firing tests which were carried out by Konštrukta-Defence a.s., Trenčín at the test institute VTSÚ Záhorie in the years 2002-2003. Ballistic data are evaluated within the quadrant elevation QE and range X according to Tab. 4. The yaw drag fitting factor Q_D and Magnus fitting factor Q_M were chosen in accordance with the US model ($Q_D = Q_M = 1{,}2$).

charge **A+A+B**			charge **D**		
QE		X	QE		X
$[mil]$	$[°]$	$[m]$	$[mil]$	$[°]$	$[m]$
366	20.6	15920	281	15.8	23184
623	35.0	20408	285	16.0	22999
686	38.6	20969	288	16.2	23588
721	40.6	20752	292	16.4	23188
994	55.9	20516	413	23.2	29089
1104	62.1	18653	483	27.2	30988
-	-	-	662	37.2	36910
-	-	-	704	39.6	37706
-	-	-	1049	59.0	37624

Tab. 4 Experimentally determined range X vs quadrant elevation QE

There was not any base burn unit ignition delay observed during the firing tests, hence the time of the base burn unit ignition delay was stated as $t_{DI} = 0\ s$. The observation of the base burn unit ignition delay was carried out by the high speed camera.

The base burn unit factor i_{BB} and lift factor f_L were analyzed by iterative algorithm, for the previously stated values of Q_D, Q_M and t_{DI}, from the results gained from the range firing tests. The base burn unit factor i_{BB} fits the range and lift factor f_L fits the side coordinate of the projectile graze. The trajectory software simulation was made for each series of rounds for the real conditions (atmospheric, ballistic and topographic) recorded during the firing. The iteration of the trajectory computation was running with the change of i_{BB} a f_L factor values till the computed graze point of the projectile was not identical with the mean point of the series of rounds. The analyzed $i_{BB}(QE)$ factor relationship is shown in Fig. 11 and the $f_L(QE)$ factor relationship in Fig. 12. Discrete points represent analyzed values from the firing tests results and the continuous curved lines represent their polynomial approximation (polynomials of the 3rd degree). As shown in Fig. 12, the values of the lift force fitting factor f_L are fairly oscillated. The oscillation mentioned above can be referred to inaccuracies in the real crosswind velocity changes evaluation. Thus, the mean value of the lift force fitting factor f_L was chosen as approximation.

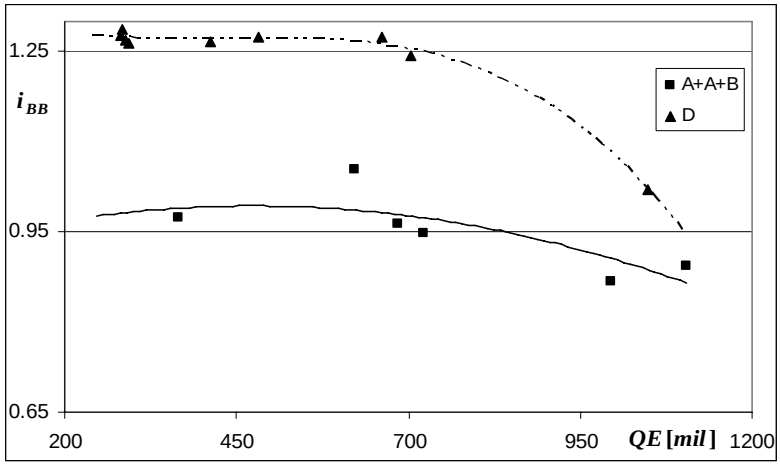

Fig. 11 Base burn unit factor i_{BB} as a function of a quadrant elevation QE

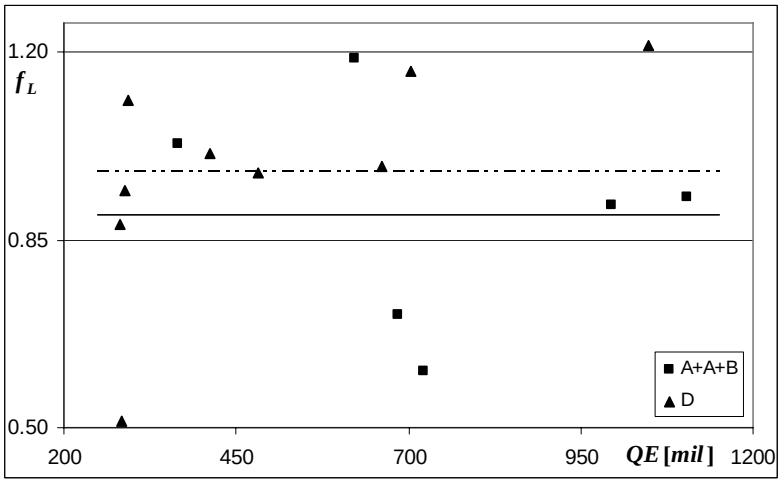

Fig. 12 Lift factor f_L as a function of a quadrant elevation QE

5. Elements of the 155 mm ERFB/BB projectile trajectory

The following elements of a standard trajectory are computed from the ballistic data analyzed for the 155 mm ERFB/BB projectile above:

- range X [m],
- velocity at graze V_ω [$m.s^{-1}$],
- total time of flight T [s],
- drift A_D [mil],
- angle of fall A_ω [°],
- trajectory vertex height Y_S [m].

The elements of a standard trajectory are computed for the following standard atmospheric, ballistic and geophysical conditions: ICAO standard atmosphere, initial speed of the projectile has the standard muzzle velocity value, initial fuzed projectile mass has the reference value, the gravitational acceleration at the mean sea level has a value related to the north latitude of 45°, i.e. $g_o = 9.80665\ m.s^{-2}$. The barrel muzzle and the point of graze lie at the mean sea level, the Coriolis force equals to zero. The elements of standard trajectory are as a function of a quadrant elevation *QE* listed in Tab. 5.

charge **A+A+B**							charge **D**						
QE [mil]	X [m]	A_D [mil]	Y_S [m]	V_ω [m/s]	A_ω [°]	T [s]	QE [mil]	X [m]	A_D [mil]	Y_S [m]	V_ω [m/s]	A_ω [°]	T [s]
100	6320	2	171	463	6,9	11,9	100	12195	3	349	559	7,9	17,0
200	10656	4	625	367	15,9	22,7	200	18971	6	1221	381	20,1	32,1
300	13762	7	1296	324	26,1	32,7	300	23496	9	2462	332	33,3	45,6
400	16126	9	2137	321	35,0	41,8	400	27153	12	4002	331	43,7	58,0
500	17996	11	3112	325	42,3	50,3	500	30384	15	5804	336	51,6	70,0
600	19444	14	4188	330	48,3	58,3	600	33311	19	7840	345	57,3	81,7
700	20463	17	5334	334	53,6	66,0	700	35843	23	10068	360	61,1	92,9
800	20994	20	6520	338	58,1	73,4	800	37736	28	12420	380	63,9	103,4
833	21032	21	6915	339	59,6	75,7	894	38477	34	14654	398	66,0	112,4
900	20872	24	7714	342	62,3	80,2	900	38473	35	14794	399	66,1	113,0
1000	19973	31	8870	347	66,2	86,4	1000	37303	43	17031	416	68,7	121,2
1100	18187	41	9938	351	70,1	91,7	1100	34061	55	18947	429	71,5	127,7
1150	16947	49	10421	353	72,1	94,0	1150	31494	70	19727	434	73,3	130,2

Tab. 5 Elements of a standard trajectory for the 155 mm ERFB/BB projectile with charges A+A+B, D

For comparison of the range obtained under the standard conditions by the 155 mm ERFB/BB projectile and the 155 mm ERFB/BT projectile (projectile with a hollow base), there is a range *X* vs quadrant elevation *QE* relationship shown in Fig. 13 for the long-range charge D. From the relationship follows that the increase of the maximal range of the 155 mm ERFB/BB projectile in comparison with the 155 mm ERFB/BT projectile is 24.5 %. The graph of a standard trajectory $O(X_1, X_2)$ of the 155 mm ERFB/BB and ERFB/BT projectiles fired with the long-range charge D on a maximal range is shown in Fig. 14.

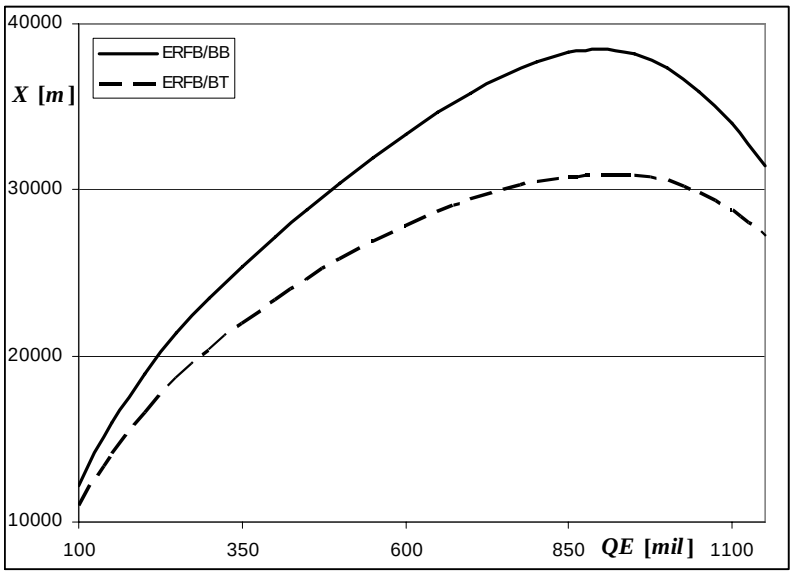

Fig. 13 Comparison of a range *X* as a function of a quadrant elevation *QE* for the 155 mm ERFB/BB and ERFB/BT projectiles fired under the standard conditions with the charge D. Optimal quadrant elevation for the ERFB/BB is of 894 *mil* (50,3°) and for the ERFB/BT is of 912 *mil* (51,3°)

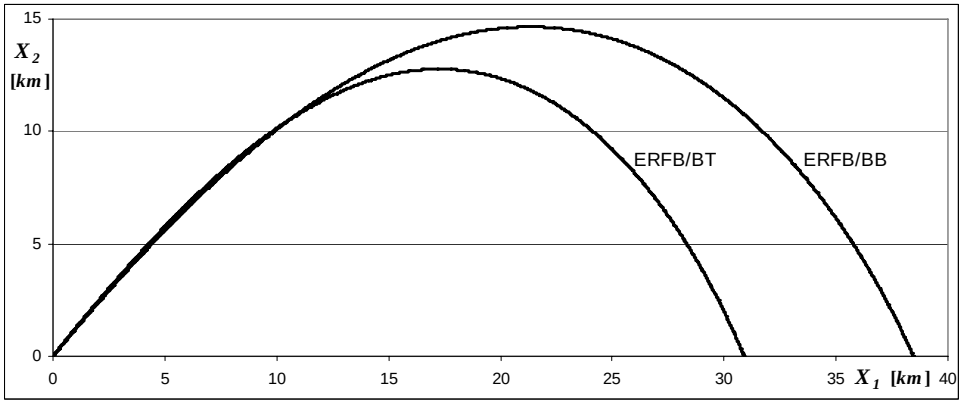

Fig. 14 Standard trajectory of the 155 mm ERFB/BB and ERFB/BT projectiles fired with long-range charge D on the maximal range

6. Conclusion

The presented trajectory model proved applicability by the trajectory modeling of the selected projectiles of a 155 mm caliber and achieved results correspond with reality. The noticeable effect of the base burn unit was proved by attacking the range limit of 40 *km* which has been considered as unrealistic for the guns of 155 mm caliber short time ago.

In the future, it will be necessary to particularize the predicted aerodynamic data in accordance with a newly developed NATO alliance publication AOP-53 "*NATO sharable software for the determination of aerodynamic coefficients*" which will be promulgated during 2006. It will be also desirable to perform the range firing tests of the ammunition with the 155 mm ERFB/BB projectile and the long-range propelling charge D in high angles of a quadrant elevation which will contribute to particularize the ballistic data.

R e f e r e n c e s :

[1] Eitemiller R. C.: Determination of Ballistic Performance Parameters for the 155 mm M864 Base-Burn Projectile. FTB-IR-9, Aberdeen Proving Ground, Maryland, 1994.

[2] Komenda J.: Základy vnější balistiky. S-999, Military Academy, Brno 2001.

[3] Lieske R. F., Danberg J. E.: Modified Point Mass Trajectory Simulation for Base-Burn Projectiles. BRL-TR-3321, Aberdeen Proving Ground, Maryland, 1992.

[4] Moss G. M., Leeming D. W., Farrar C. L.: Military Ballistics. Brassey's (UK) Ltd, London 1995.

[5] STANAG 4355, Edition 2 and Draft Edition 4: Modified Point Mass and Five Degrees of Freedom Trajectory Models.

[6] Textbook of Ballistics and Gunnery, Volumes I and II. Her Majesty's Stationary Office, London 1987.